

Off-shell pairing correlations from meson-exchange theory of nuclear forces

A. Sedrakian

Institut für Theoretische Physik, Universität Tübingen, D-72076 Tübingen, Germany

(Dated: May 22, 2019)

Abstract

A model is developed for treating off-mass-shell pairing correlations in nuclear systems. These correlations are described by a coupled set of meson-exchange normal and anomalous Fock self-energies of baryons. The kernel of the complex gap equation for baryons is related to the in-medium spectral function of mesons, which is evaluated non-perturbatively in the random phase approximation. The model is applied to the low density neutron matter in neutron star crusts by modeling the interaction as a sum of a long-range one-pion exchange component and a short range component parameterized in terms of Landau Fermi-liquid parameters. An efficient algorithm is described for the self-consistent solution of the resulting Eliashberg type non-linear integral equations. We find that the off-shell pairing correlations extend to rather high energies – of the order of 100 MeV – with the real and imaginary parts of the pairing gap showing a complicated structure. At low energies the damping of the neutron pair correlations due to the coupling to the pionic modes is small, but becomes increasingly important, and eventually dominant as the energy is increased.

I. INTRODUCTION

The lowest order in the interaction mean-field treatments of the nuclear pairing in bulk nuclear matter and in finite nuclei are conceptually simple and have been reasonably consistent with the phenomenology of these systems. The Hartree-Fock-Bogolyubov (HFB) theory with zero- or finite-range (e.g. the Skyrme and the Gogny) phenomenological forces has been the standard tool in the studies of the nuclear structure to described the bulk of the experimental data [1]. At the same time, the calculations of the pairing gaps in the infinite matter based on the Bardeen-Cooper-Schrieffer (BCS) theory with interactions modeled by the bare (realistic) nucleon-nucleon forces and quasiparticle spectra in the effective mass approximation are not inconsistent with the cooling simulations of neutron stars or the phenomenology of their rotation dynamics. Although there is no direct evidence for higher order correlations in the phenomenology of nuclear systems, these can not be discarded on the basis of purely phenomenological arguments. First, the effective forces used in the HFB calculations are fit to the pairing properties of (some) nuclei, consequently the contributions beyond mean field are built-in automatically (e.g. the effective Skyrme or Gogny forces include the contributions from the ladder diagrams). Second, the values of the pairing gaps deduced from the phenomenology of neutron stars depend sensitively on the physical input, such as the equation of state, the matter composition, and its dynamical properties. Provided the uncertainties in these ingredients the phenomenological values of the gap can be off by an order of magnitude. From the theory point of view the higher order correlations might not be manifest due to large cancellation between the vertex and propagator renormalization. This is an open issue, since the pairing properties are sensitive to the details of the renormalization procedure and definitive conclusions about the cancellations can be gained from the theories which fulfill a number of general constraints such as the Ward-identities, the spectral sum rules, etc.

The on-mass-shell behavior of the pairing amplitude (gap function) is well understood: its momentum dependence is controlled by the shape of the diagonal in momenta matrix element of the (effective) nuclear interaction in a fixed partial-wave channel. Although the contribution of the high-momentum modes can not be neglected, the kernel of the BCS gap equation is sharply peak at the Fermi energy, and the magnitude of the gap is controlled by the propagator and vertex renormalizations at the Fermi surface. The early work to con-

struct renormalization schemes for strongly interacting fermions introduced wave-function renormalization factors in the kernel of the gap equation and modeled the effective pairing interaction in terms of particle-hole irreducible vertices [2]. These were related to the phenomenological Landau Fermi-liquid parameters which can (in principle) be fixed by a comparison with the experiments. The Landau parameters can also be obtained from ab initio microscopic calculations which are needed for example to describe isospin asymmetric nuclear systems that are not directly accessible in the laboratories [3, 4]. Subsequent work on the pairing in the infinite matter beyond the mean-field (BCS) approximation concentrated on various aspects of the problem. This work includes the microscopic calculations of the effective interactions and Landau effective masses using variants of the Babu-Brown [5] or related schemes of summing the polarization graphs in neutron matter [6, 7]; the correlated basis variational theories based on the Jastrow ansatz for fermionic wave-functions [8]; the calculations which include the wave-function renormalization constructed from the self-energies derived either from the Brueckner theory or the scattering t -matrix [9]; the calculations based on the Thouless criterion for the scattering t -matrix [10]; the theories motivated by the renormalization group approach to construct effective interactions [11, 12]; the self-consistent propagator and vertex renormalization calculations using the effective Gogny interactions [13]. There is general agreement that the vertex corrections and propagator renormalizations reduce the mean-filed BCS value of the on-shell pairing gap by a factor of four or so.

The off-mass-shell physics of the nuclear pairing is much less understood. The corresponding contributions to the (complex) pairing amplitude are generated by time non-local interactions and this requires an appropriate choice of the bosonic degrees of freedom that contribute dominantly to the retarded interactions. The generic theory of the boson-exchange superconductors is known in the form first developed by Eliashberg [14] to describe the superconductivity in materials where the electron-phonon coupling is of the order of unity. However, Eliashberg's theory rests on the Migdal theorem, which permits to keep only the leading order term in the expansion of the electron-phonon vertex with respect to a small expansion parameter – the ratio of the phonon Debye energy to the Fermi energy of electrons. Clearly, neither the baryon-meson interaction vertex is weak nor the meson self-energies can be treated in the perturbation theory and the common form of the theory is not applicable in our context. The off-shell effects induced by retarded interactions and the corresponding

strong coupling equations have been discussed previously in Refs. [15, 16, 17]. In the context of laboratory nuclei the retarded pairing interaction is driven by an exchange of the virtual phonons - low-lying collective bosonic excitation [16, 17]. In the astrophysical context of neutron star crusts the attractive pairing interaction is mediated by an exchange of *real* phonons of the nuclear Coulomb lattice of the crusts [15].

We argue below that the renormalized pionic (and more generally mesonic) modes provide the dominant contribution to the retarded nuclear interactions in infinite nuclear/neutron matter and show that the resulting off-shell pairing correlations extend up to frequencies ~ 100 MeV. These frequencies are an order of magnitude larger than those deduced for phonon-exchange models. The retarded pairing interaction is approximated below by a dressed one-boson exchange among baryons. Thus, unlike the potential models, it incorporates the medium modification of the dispersion relation of the mesons. Of course, the meson exchange picture of pairing is known in the form that emerged during the last decade in the context relativistic mean-field theories [18]. However the predictive power of the Hartree models is limited, since there is no natural cut-off in the theory (and the theory is non-renormalizable). No attempts have been made to access the off-shell behavior of the pairing gaps from the relativistic Fock self-energies so far.

The self-energies and the vertex corrections in our model are treated on the same footing within the Random-Phase-Approximation (RPA). The non-perturbative resummation of the particle-hole diagrams in the RPA is carried out in the spirit of Migdal's theory of finite Fermi systems by modeling the residual interaction in terms of a contact approximation to the g' Landau parameter. The retardation effects are induced by the Fock (exchange) contributions to the self-energies of baryons. The resulting off-mass-shell behavior of the gap function is determined self-consistently by coupled integral equations for an energy dependent complex gap function and a complex wave-function renormalization.

To elucidate our approach we start with the π_0 -exchange interaction among neutrons in a low density neutron matter relevant for the physics of neutron star crusts. In the density regime $(0.002 - 0.5) \times \rho_0$, where $\rho_0 = 0.17 \text{ fm}^{-3}$ is the nuclear saturation density, the matter in neutron stars is an admixture of unbound neutron liquid and a Coulomb lattice of nuclei with a charge-neutralizing background of relativistic electrons [19, 20, 21]. The temperatures are much smaller than the typical Fermi energies and the neutrons form a zero-temperature Fermi-liquid. Low temperatures constrain the particles to lie close to their Fermi surface,

while the physics off the mass-shell is essentially unconstrained by the degeneracy of the system. It appears then appropriate to restrict the momenta of quasiparticles to their Fermi surface and treat exactly the frequency-dependence of the propagators and effective interactions. The corresponding quasi-classical (or Eliashberg) Green's functions are obtained by integrating out the on-shell energy variable of the original Green's functions, but keeping the full frequency dependence of the propagators. Our numerical calculations below are carried out in this limit.

The remainder of the paper is organized as follows. In Sec. II we describe the essentials of the model in the framework of the real time Green's functions formalism. A detailed exposition will be given elsewhere. Sec. III presents the numerical algorithm developed for the solution of the coupled non-linear integral equations. The results are discussed for the case under study – the pairing in the low-density neutron matter – where the retarded pairing interaction is mediated by an exchange of neutral pions. Sec. IV contains our conclusions.

II. MODEL

Below the model is formulated in terms of the real-time contour-ordered Green's functions [22]. The imaginary time Matsubara formalism is well suited for our purposes, since we treat systems in equilibrium, however, the numerical solutions of the equations formulated on the real frequency axis are technically simpler compared to the solution of the imaginary time equations. The latter require a summation of finite number of discrete Matsubara frequencies with a certain cut-off frequency which is followed by an analytical continuation to the real axis; the former are solved directly on the real axis.

The real-time treatment of the superfluid system requires a 4×4 matrix structure of the propagators and self-energies in general [22]. A 2×2 matrix structure is due to the time ordering of the propagators on the real-time contour (Keldysh matrix); and a 2×2 structure is needed to account for the anomalous correlation due to the pairing (Nambu-Gor'kov matrix). The components of the Nambu-Gor'kov matrix obey the following coupled

Dyson equations

$$\hat{G}_{\alpha\beta}(p) = \hat{G}_{0\alpha\beta}(p) + \hat{G}_{0\alpha\gamma}(p) \left[\hat{\Sigma}_{\gamma\delta}(p) \hat{G}_{\delta\beta}(p) + \hat{\Delta}_{\gamma\delta}(p) \hat{F}^\dagger_{\delta\beta}(p) \right], \quad (1)$$

$$\hat{F}^\dagger_{\alpha\beta}(p) = \hat{G}_{0\alpha\gamma}(-p) \left[\hat{\Delta}_{\gamma\delta}^\dagger(p) \hat{G}_{\delta\beta}(p) + \hat{\Sigma}_{\gamma\delta}(-p) \hat{F}^\dagger_{\delta\beta}(p) \right], \quad (2)$$

$$\hat{F}_{\alpha\beta}(p) = \hat{G}_{0\alpha\gamma}(p) \left[\hat{\Delta}_{\gamma\delta}(p) \hat{G}_{\delta\beta}(-p) + \hat{\Sigma}_{\gamma\delta}(p) \hat{F}_{\delta\beta}(p) \right], \quad (3)$$

$$\hat{G}_{\alpha\beta}(-p) = \hat{G}_{0\alpha\beta}(-p) + \hat{G}_{0\alpha\gamma}(-p) \left[\hat{\Sigma}_{\gamma\delta}(-p) \hat{G}_{\delta\beta}(-p) + \hat{\Delta}_{\gamma\delta}^\dagger(p) \hat{F}_{\delta\beta}(p) \right], \quad (4)$$

where $\hat{G}_{\alpha\beta}(p)$ and $\hat{G}_{0\alpha\beta}(p)$ are the full and free normal propagators, $\hat{F}^\dagger_{\alpha\beta}(p)$ and $\hat{F}_{\alpha\beta}(p)$ are the anomalous propagators, and $\hat{\Sigma}_{\alpha\beta}(p)$ and $\hat{\Delta}_{\alpha\beta}(p)$ are the normal and anomalous self-energies; p denotes the four-momentum, the Greek subscripts are the spin/isospin indeces; summation over repeated indeces is understood. The hat indicates that the propagators and self-energies are contour order, i.e. are 2×2 matrices in the Keldysh space. We shall assume that the interactions conserve spin and isospin, i.e. $\hat{G}_{\alpha\beta}(p) = \delta_{\alpha\beta} \hat{G}(p)$ and $\hat{\Sigma}_{\alpha\beta}(p) = \delta_{\alpha\beta} \hat{\Sigma}(p)$ and concentrate below on the pairing in the state of total spin $S = 0$, total isospin $I = 1$, and orbital angular momentum $L = 0$. Thus the anomalous propagators and self-energies must be antisymmetric with respect to the spin indeces and symmetric in the isospin indeces

$$\hat{F}^\dagger_{\alpha\beta}(p) = g_{\alpha\beta} \hat{F}^\dagger(p) \quad \hat{F}_{\alpha\beta}(p) = g_{\alpha\beta} \hat{F}(p) \quad (5)$$

$$\hat{\Delta}_{\alpha\beta}^\dagger(p) = g_{\alpha\beta} \hat{\Delta}^\dagger(p), \quad \hat{\Delta}_{\alpha\beta}(p) = g_{\alpha\beta} \hat{\Delta}(p), \quad (6)$$

where $g_{\alpha\beta} \equiv i\sigma_y$ is the spin matrix with σ_y being the second component of the vector Pauli matrices; the unit matrix in the isospin space is suppressed. The Dyson Eqs. (1)-(4) can be written in terms of auxiliary Green's functions, which describe the unpaired state of the system

$$\hat{G}_{\alpha\beta}^N(p) = \hat{G}_{0\alpha\beta}(p) + \hat{G}_{\alpha\beta}^N(p) \hat{\Sigma}_{\gamma\delta}(p) \hat{G}_{0\alpha\beta}^N(p), \quad (7)$$

$$\hat{G}_{\alpha\beta}^N(-p) = \hat{G}_{0\alpha\beta}(-p) + \hat{G}_{\alpha\beta}^N(-p) \hat{\Sigma}_{\gamma\delta}(-p) \hat{G}_{0\alpha\beta}^N(-p). \quad (8)$$

Combining Eqs. (1)-(4) and (7)-(8) we find an equivalent form of the Dyson equations:

$$\hat{G}_{\alpha\beta}(p) = \hat{G}_{\alpha\gamma}^N(p) \left[\delta_{\gamma\beta} + \hat{\Delta}_{\gamma\delta}(p) \hat{F}^\dagger_{\delta\beta}(p) \right], \quad (9)$$

$$\hat{F}^\dagger_{\alpha\beta}(p) = \hat{G}_{\alpha\gamma}^N(-p) \hat{\Delta}_{\gamma\delta}^\dagger(p) \hat{G}_{\alpha\beta}(p), \quad (10)$$

$$\hat{F}_{\alpha\beta}(p) = \hat{G}_{\alpha\gamma}^N(p) \hat{\Delta}_{\gamma\delta}(p) \hat{G}_{\alpha\beta}(-p), \quad (11)$$

$$\hat{G}_{\alpha\beta}(-p) = \hat{G}_{\alpha\gamma}^N(-p) \left[\delta_{\gamma\beta} + \hat{\Delta}_{\gamma\delta}^\dagger(p) \hat{F}_{\delta\beta}(p) \right]. \quad (12)$$

The time-reversal symmetry implies that $\Delta_{\alpha\beta}(p) = [\Delta_{\alpha\beta}^\dagger(p)]^*$, i.e. the pairing correlations in the system are fully specified if we know one of the two anomalous Green's functions; in other words it is sufficient to solve Eq. (9) with either Eq. (10) or (11). If we are interested in the equilibrium properties of the system it is convenient to solve the Eqs. (9)-(12) for the retarded propagators. The form of these equations remains the same as we replace the contour ordered functions by the retarded (more precisely the contour ordered Dyson equation is invariant under a class of unitary transformations which bring the Keldysh matrix to the so-called ‘triangular’ form in which the diagonal elements are the retarded and advanced propagators [22]). We first substitute in Eqs. (7)-(8) for the normal state retarded propagators $G_{\alpha\beta}^{N,R}(\pm p) = \delta_{\alpha\beta}[\pm(\omega + i\eta) - \xi_p - \Sigma^R(\pm p)]^{-1}$, where ξ_p is the free quasiparticle spectrum in the normal state. After decomposing the retarded self-energy into the even and odd in ω components, $\Sigma^R(p) = \Sigma_S^R(p) + \Sigma_A^R(p)$, we further define the wavefunction renormalization $Z(p) = 1 - \omega^{-1}\Sigma_A^R(p)$ and the renormalized quasiparticle spectrum $\xi_p^* = \xi_p + \Sigma_S^R(\mathbf{p}, \xi_p^*)$. Then, the solution of algebraic equations (9) and (11) is

$$G^R(p) = \frac{\omega Z(p) + \xi_p^*}{\omega^2 Z(p)^2 - \xi_p^{*2} - \Delta^R(p)^2 + i\eta}, \quad (13)$$

$$F^R(p) = -\frac{\Delta^R(p)}{\omega^2 Z(p)^2 - \xi_p^{*2} - \Delta^R(p)^2 + i\eta}, \quad (14)$$

where we used the fact that $\Delta_{\alpha\beta}\Delta_{\beta\gamma}^\dagger = -\Delta^2$. For the purpose of analytical representation Feynman diagrams for the self-energies it is convenient to introduce additional real-time Green's functions by the relations

$$G^{>,<}(p) = iA_G(p)f^{>,<}(\omega), \quad (15)$$

$$F^{>,<}(p) = iA_F(p)f^{>,<}(\omega), \quad (16)$$

where $A_G(\omega)$ and $A_F(\omega)$ are the normal and anomalous spectral functions, $f^{>,<}(\omega)$ are Wigner distribution functions. In non-equilibrium theory these propagators are the off-diagonal elements of the Keldysh matrix (i.e. have their time arguments on the opposite branches of the time-contour) and are the solutions of transport equations. However in equilibrium the relations (15) and (16) do not contain additional information, for the spectral functions $A_G(\omega)$ and $A_F(\omega)$ can be related to the retarded propagators by the their spectral

representation (here we dropped the three-momentum dependence of the functions)

$$G^R(\omega) = \int_{-\infty}^{\infty} \frac{d\varepsilon}{2\pi} \frac{A_G(\varepsilon)}{\omega - \varepsilon + i\eta}, \quad (17)$$

$$F^R(\omega) = \int_{-\infty}^{\infty} \frac{d\varepsilon}{2\pi} \frac{A_F(\varepsilon)}{\omega - \varepsilon + i\eta}, \quad (18)$$

and the Wigner distribution functions reduce to the Fermi-distribution functions for particles and holes: $f^<(\omega) \equiv f(\omega) = [\exp(\beta\omega) + 1]^{-1}$ and $f^>(\omega) = f(\omega) - 1$, where β is the inverse temperature. In other words, the relations (15) and (16) establish a one-to-one correspondence between the retarded and $G^{>,<}(p)$, $F^{>,<}(p)$ propagators. Our final equations will be given in terms of the quasiclassical (Eliashberg) propagators where the quasi-particle momenta are restricted to their Fermi-surfaces. These propagators are defined by integrating out the on-shell momentum dependence of the retarded propagators:

$$G^Q(\omega) = \int_{-\infty}^{\infty} d\xi_p^* G^R(\mathbf{p}, \omega), \quad (19)$$

$$F^Q(\omega) = \int_{-\infty}^{\infty} d\xi_p^* F^R(\mathbf{p}, \omega). \quad (20)$$

To model the interaction, we separate its long-range and short-range components. The long-range part is modeled in terms of the one-pion-exchange (OPE) potential; the short range correlations are parameterized in terms of a few Landau parameters, as is commonly done in the theory of finite Fermi-systems [23, 24]. The OPE interaction among neutrons in the momentum space is given by (our conventions follow Ref. [23])

$$V_\pi(\mathbf{q}) = -\frac{1}{3} \frac{f_\pi^2}{m_\pi^2} \frac{\mathbf{q}^2}{\mathbf{q}^2 + m_\pi^2} [(\boldsymbol{\sigma}_1 \cdot \boldsymbol{\sigma}_2) + S_{12}(\mathbf{n})] \boldsymbol{\tau}_1 \cdot \boldsymbol{\tau}_2, \quad (21)$$

where f_π is the pion-nucleon coupling constant, m_π is the pion mass, $\boldsymbol{\sigma}$ and $\boldsymbol{\tau}$ are the vectors of Pauli-matrices in the spin and isospin spaces, indeces 1 and 2 refer to the particles, \mathbf{q} is the momentum transfer, $\mathbf{n} = \mathbf{q}/q$, and $S_{12}(\mathbf{n})$ is the tensor operator. The short range correlations are given by [23]

$$V_{\text{corr}}(\omega, q) = \frac{f_\pi^2}{m_\pi^2} [g'(\omega, q) \boldsymbol{\sigma}_1 \cdot \boldsymbol{\sigma}_2 + h'(\omega, q) \boldsymbol{\sigma}_1 \cdot \boldsymbol{\sigma}_2 S_{12}(\mathbf{n})] \boldsymbol{\tau}_1 \cdot \boldsymbol{\tau}_2, \quad (22)$$

where g' and h' are the dimensionless Landau parameters. Eq. (22) contains only the spin-isospin part of the parameterization of the short-range part of the interaction in terms of the Landau parameters relevant for the RPA renormalization of the vertices and the polarization tensor. Furthermore, we shall keep below only the contribution from the g' parameter and

approximate it by a constant value $g' = 0.6$ [23]. The full meson propagator obeys the Dyson equation

$$\hat{D}(p) = \hat{D}_0(p) + \hat{D}_0(p)\hat{\Pi}(p)\hat{D}(p), \quad (23)$$

where $\hat{D}_0(q)$ is the free meson propagator and the polarization tensor is defined as

$$\hat{\Pi}(q) = -\text{Tr} \int \frac{d^4 p}{(2\pi)^4} \hat{\Gamma}_0(q) \hat{G}(p+q) \hat{G}(-p) \hat{\Gamma}(q), \quad (24)$$

where $\hat{\Gamma}_0(q)$ and $\hat{\Gamma}(q)$ are the bare and full pion-nucleon vertices. The former can be read-off from the one-pion exchange potential (21). The full pion-nucleon vertex is defined by the integral equation

$$\hat{\Gamma}(q) = \hat{\Gamma}_0(q) + \text{Tr} \int \frac{d^4 p}{(2\pi)^4} \hat{\Gamma}_1(q) \hat{G}(p+q) \hat{G}(-p) \hat{\Gamma}(q), \quad (25)$$

where $\hat{\Gamma}_1(q)$ is the short-range part of the particle-hole interaction which can be approximated by Eq. (22). In general the propagators in Eq. (24) and (25) are 2×2 matrices in the Nambu-Gor'kov space. The contributions from the anomalous sector, however, involve propagator products which contain powers of F , each contributing a suppression factor $\mathcal{O}(\Delta/\mu)$, where μ is the Fermi energy. Therefore, we shall keep below only the contribution from the non-superconducting propagators to the polarization tensor, which means that the renormalization of the pion dispersion relation is carried out in the normal state. As in the baryon sector, we introduce the pion Green's functions $D^{>,<}(q)$, which are the off-diagonal elements of the non-equilibrium matrix propagator (i.e. have their time arguments on the opposite branches of the time-contour) by the relations

$$D^<(q) = -iB(q)g(\omega) - iB(-q)[1 + g(\omega)], \quad (26)$$

$$D^>(q) = -iB(q)[1 + g(\omega)] - iB(-q)g(\omega), \quad (27)$$

where $g(\omega) = [\exp(\beta\omega) - 1]^{-1}$ is the Bose distribution function and $B(q)$ is the pion spectral function. The latter is related to the retarded component of the polarization tensor Eq. (24) by the relation

$$B(q) = \frac{-2\text{Im}\Pi^R(q)}{[\omega^2 - \mathbf{q}^2 - m_\pi^2 - \text{Re}\Pi^R(q)]^2 + [\text{Im}\Pi^R(q)]^2}. \quad (28)$$

The one loop-polarization tensor for neutral pions in a non-interacting neutron gas at zero temperature is given by

$$\Pi_0^R(\omega, q) = -\frac{2f_\pi^2 q^2}{m_\pi^2} \phi_L(\omega, q), \quad (29)$$

where $\phi_L(\omega, q)$ is the Lindhard function. The RPA renormalization of the polarization tensor then leads to

$$\Pi^R(\omega, q) = -\frac{2f_\pi^2 q^2}{m_\pi^2} \left[1 - \frac{2f_\pi^2}{m_\pi^2} g' \phi_L(\omega, q) \right]^{-1} \phi_L(\omega, q). \quad (30)$$

The form of the polarization tensor thus completely determines the spectral function of pions, which is the central quantity for the calculations of the pairing self-energies.

The time non-local normal and anomalous self-energies are given by the Fock diagrams of the generic form

$$\hat{\Sigma}(p) = - \int \frac{d^4 q}{(2\pi)^4} \hat{\Gamma}_{0\pi}(q) \hat{D}(q) \hat{G}(p - q) \hat{\Gamma}_\pi(q), \quad (31)$$

$$\hat{\Delta}(p) = - \int \frac{d^4 q}{(2\pi)^4} \hat{\Gamma}_{0\pi}(q) \hat{D}(q) \hat{F}(p - q) \hat{\Gamma}_\pi(-q). \quad (32)$$

Since only the central part of the interaction contributes to the pairing interaction in the $S = 0, I = 1$ state we drop the tensor term $\propto S_{12}(\mathbf{n})$ and put $(\boldsymbol{\sigma}_1 \cdot \boldsymbol{\sigma}_2)(\boldsymbol{\tau}_1 \cdot \boldsymbol{\tau}_2) = -3$ in the OPE potential (21). To obtain the full pairing vertex we use the same renormalization procedure as for the polarization tensor to include the effects of the short range correlations. In addition, the vertex correction should include diagrams which iterate the pion exchange at the full vertex. This could be achieved by a redefinition of the parameter g' [24] if the pairing correlations in the full vertex can be neglected; we do not treat the pion-mediated vertex corrections in the following. Figure 1 shows the Feynman diagrams corresponding to Eqs. (31) and (32). The analytical expressions for the retarded components of the self-energies can be read-off from the diagrams

$$\begin{aligned} \Sigma^R(\omega) &= \int_{-\infty}^{\infty} \frac{d\bar{\omega}}{2\pi} \frac{\Sigma^>(\bar{\omega}) - \Sigma^<(\bar{\omega})}{\omega - \bar{\omega} + i\eta}, \\ &= \int_{-\infty}^{\infty} \frac{d\bar{\omega}}{2\pi} \int_0^{\infty} \frac{d\omega'}{2\pi} \frac{D^>(\omega') G^<(\bar{\omega} - \omega') - D^<(\bar{\omega}) G^>(\bar{\omega} - \omega')}{\omega - \bar{\omega} + i\eta}, \end{aligned} \quad (33)$$

$$\begin{aligned} \Delta^R(\omega) &= \int_{-\infty}^{\infty} \frac{d\bar{\omega}}{2\pi} \frac{\Delta^>(\bar{\omega}) - \Delta^<(\bar{\omega})}{\omega - \bar{\omega} + i\eta} \\ &= \int_{-\infty}^{\infty} \frac{d\bar{\omega}}{2\pi} \int_0^{\infty} \frac{d\omega'}{2\pi} \frac{D^>(\omega') F^{\dagger<}(\bar{\omega} - \omega') - D^<(\bar{\omega}) F^{\dagger>}(\bar{\omega} - \omega')}{\omega - \bar{\omega} + i\eta}, \end{aligned} \quad (34)$$

where we used the dispersion relations for the retarded self-energies $\Sigma^R(\omega)$ and $\Delta^R(\omega)$ [in Eqs. (33) and (34) the momentum variables and the vertices have been suppressed]. Substituting the spectral representations of the Green's functions in the above expression we

arrive at

$$\Sigma^R(\omega, \mathbf{p}) = \int \frac{d^3 q}{(2\pi)^3} \int_{-\infty}^{\infty} \frac{d\varepsilon}{2\pi} \Gamma_{0\pi}(\mathbf{q}) A_G(\varepsilon, \mathbf{p} - \mathbf{q}) C(\omega, \varepsilon, \mathbf{q}) \Gamma_{\pi}(\mathbf{q}), \quad (35)$$

$$\Delta^R(\omega, \mathbf{p}) = \int \frac{d^3 q}{(2\pi)^3} \int_{-\infty}^{\infty} \frac{d\varepsilon}{2\pi} \Gamma_{0\pi}(\mathbf{q}) A_F(\varepsilon, \mathbf{p} - \mathbf{q}) C(\omega, \varepsilon, \mathbf{q}) \Gamma_{\pi}(\mathbf{q}), \quad (36)$$

where

$$C(\omega, \varepsilon, \mathbf{q}) = \int_0^{\infty} \frac{d\omega'}{2\pi} B(\omega', \mathbf{q}) \left[\frac{f(\varepsilon) + g(\omega')}{\omega - \omega' - \varepsilon + i\eta} + \frac{1 - f(\varepsilon) + g(\omega')}{\omega + \omega' - \varepsilon + i\eta} \right]. \quad (37)$$

Equations (35)-(37) for the Fock self-energies are still rather general, for the approximations to the spectral function of pions and the pion-nucleon vertices have not been specified. In the numerical computations we shall use the RPA renormalized spectral function of pions and the one-pion exchange vertices which are dressed by the short-range correlations. We now turn to the kinematical restriction on the momentum variables in Eqs. (35)-(37). These are non-linear coupled integral equation of four variables (three components of the momentum transfer and the energy) in general. As discussed in the introduction, for systems with a well-defined Fermi surface it is justified to restrict the momenta of the interacting particles to their Fermi surfaces, since the kernels of the integral equations are sharply peaked at the Fermi momentum. This is the essential approximation of the model which (in line with the standard from of the Eliashberg theory) eliminates the momentum dependence of the propagators and self-energies. Upon carrying out the integrations over the on-mass-shell energy in Eqs. (35) and (36), which convert the retarded Green's functions into their quasi-classical counterparts, we obtain

$$\begin{aligned} \Sigma^Q(\omega) = & - \int_0^{\infty} d\omega' K(\omega') \left\{ i\pi g(\omega') [G^Q(\omega + \omega') - G^Q(\omega - \omega')] \right. \\ & \left. + \int_{-\infty}^{\infty} d\varepsilon \text{Re} [G^Q(\varepsilon)] \left[\frac{f(\varepsilon)}{\varepsilon - \omega + \omega' - i\eta} + \frac{1 - f(\varepsilon)}{\varepsilon - \omega - \omega' - i\eta} \right] \right\}, \end{aligned} \quad (38)$$

$$\begin{aligned} \Delta^Q(\omega) = & \frac{1}{Z(\omega)} \int_0^{\infty} d\omega' K(\omega') \left\{ i\pi g(\omega') [F^Q(\omega + \omega') - F^Q(\omega - \omega')] \right. \\ & \left. + \int_{-\infty}^{\infty} d\varepsilon \text{Re} [F^Q(\varepsilon)] \left[\frac{f(\varepsilon)}{\varepsilon - \omega + \omega' - i\eta} + \frac{1 - f(\varepsilon)}{\varepsilon - \omega - \omega' - i\eta} \right] \right\}, \end{aligned} \quad (39)$$

where $\Sigma^Q(\omega)$ and $\Delta^Q(\omega)$ are the quasi-classical counterparts of the retarded self-energies and we defined the momentum averaged effective interaction kernel by

$$K(\omega) = \frac{m^*}{(2\pi)^3 p_F} \int_0^{2p_F} dq q \int_0^{2\pi} d\varphi \Gamma_{0\pi}(\mathbf{q}) B(\mathbf{q}, \omega) \Gamma_{\pi}(\mathbf{q}), \quad (40)$$

where p_F is the Fermi momentum; note that the function $K(\omega)$ is real. Eqs. (38)-(39) are coupled non-linear integral equations for the complex pairing amplitude and the normal self-energy (i.e. are equivalent to four integral equations for four real quantities). The driving term of the interaction kernel is given by the momentum averaged spectral function of pions which includes the effects of the modification of the pionic spectrum by the nuclear medium. Note that the anomalous Hartree contribution (the tadpole diagram) should be added to the anomalous Fock self-energy in general. Approximating the time-local S -wave interaction in terms of Landau parameterization $F_0(\omega, \mathbf{q}) + G_0(\omega, \mathbf{q})(\boldsymbol{\sigma}_1 \cdot \boldsymbol{\sigma}_2)$ one finds for the mean-field BCS contribution to the pairing in the spin-zero state

$$\Delta_{BCS}^R(\omega, \mathbf{p}) = \int \frac{d^4 q}{(2\pi)^4} [F_0(\omega, \mathbf{q}) - 3G_0(\omega, \mathbf{q})] F^<(\omega + \omega', \mathbf{p} + \mathbf{q}). \quad (41)$$

If the Landau parameters are further approximated by a constant, the quasiclassical approximation to the Hartree self-energy becomes

$$\Delta_{BCS}^Q(\omega) = (F_0 - 3G_0)\nu(\mu) \int_{-\infty}^{\infty} d\omega' f(\omega') \text{Re} [F^Q(\omega + \omega')], \quad (42)$$

where $\nu(\mu)$ is the density of states per spin at the Fermi surface. Below we concentrate only on the contribution from the Fock diagrams and drop the BCS contribution to the pairing gap. In the zero temperature limit Eqs. (38)-(39) reduce to

$$Z(\omega) = 1 - \frac{1}{\omega} \int_{-\infty}^{\infty} d\varepsilon \text{Re} \left[\frac{\varepsilon}{\sqrt{\omega^2 - \Delta^Q(\varepsilon)^2}} \right] \text{sgn}(\varepsilon) L(\omega, \varepsilon), \quad (43)$$

$$\Delta^Q(\omega) = \frac{1}{Z(\omega)} \int_{-\infty}^{\infty} d\varepsilon \text{Re} \left[\frac{\Delta^Q(\varepsilon)}{\sqrt{\omega^2 - \Delta^Q(\varepsilon)^2}} \right] \text{sgn}(\varepsilon) L(\omega, \varepsilon), \quad (44)$$

where we re-introduced the wave-function renormalization $Z(\omega)$ and defined an effective (complex) retarded interaction as

$$L(\omega, \varepsilon) = \int_0^{\infty} d\omega' K(\omega') \left[\frac{\theta(-\varepsilon)}{\varepsilon - \omega + \omega' - i\eta} + \frac{\theta(\varepsilon)}{\varepsilon - \omega - \omega' - i\eta} \right], \quad (45)$$

where $\theta(\varepsilon)$ is the Heavyside's step function. Note that the thermal occupation probability of the pions vanishes in the zero temperature limit and their effect is contained entirely in the effective interaction $L(\omega, \varepsilon)$. Note also that due to the time reversal symmetry of the problem the energy integrations in Eqs. (43) and (44) can be restricted to the positive values of the energy variable upon using the property $\Delta^Q(-\varepsilon) = \Delta^Q(\varepsilon)$ and the symmetries of the effective interaction.

III. THE ALGORITHM AND RESULTS

Equations (43) and (44) form a coupled set of four nonlinear integral equations for four real functions: these are the real and imaginary parts of the gap function $\Delta_1^Q(\omega)$ and $\Delta_2^Q(\omega)$, and the real and imaginary parts of the wave-function renormalization $Z_1(\omega)$ and $Z_2(\omega)$. Since the interaction kernel $L(\omega, \varepsilon)$ is constructed from the spectral function of pions renormalized by the nuclear medium in the normal state, it serves as an input to Eqs. (43) and (44) and can be computed prior to their solution. Thus, the computational task is naturally divided into two parts. In the first part the $L(\omega, \varepsilon)$ function is generated on a two-dimensional energy grid. The starting point is the construction of the pion-spectral function from the real and imaginary parts of the the RPA renormalized polarization function. The RPA polarization function is in turn constructed from the free-particle polarization function (or the Lindhard function) which has an analytical form both at zero and finite temperatures. From the pion spectral function and the RPA-renormalized vertex $\Gamma(q)$ we then construct the momentum-averaged effective interaction $K(\omega)$ according to Eq. (40) in a typical energy range $0 \leq \omega \leq 200$ MeV. The first part of the computation is accomplished by constructing the real and imaginary parts of the function $L(\omega, \varepsilon)$ on a two-dimensional energy grid. Typical computations were carried out on a 100×100 point mesh. The energy range covered was extended up to 400 MeV to ensure that the integrands in Eqs. (43) and (44) have dropped to values below the accuracy of the integration. Note that the evaluation of Eq. (45) requires principle value integrations due to the simple poles in the integrand and, in addition, evaluation of integrals which are singular at the boundary.

In the second part of the computation the four integral equations represented by Eqs. (43) and (44) are solved self-consistently using as an input the values of the function $L(\omega, \varepsilon)$ stored on a two-dimensional energy grid. An iterative procedure is used. The iteration starts by assigning to the functions the values $\Delta_1^Q(\omega) = \Delta_{BCS}$, $\Delta_2^Q(\omega) = 0$, $Z_1(\omega) = 1$ and $Z_2(\omega) = 0$, where Δ_{BCS} is the constant BCS value of the pairing gap for $\omega = 0$. The newly computed functions are reinserted in the kernels on the right-hand side of the equations and the iterations are repeated until a convergence is achieved. Note that the kernels of Eqs. (43) and (44) are singular; in the first of these equations the singularity is always at the lower boundary of the integration region, while in the second equation singularities occurs both at the lower end-point and within the integration regions (the latter should be understood

in the Cauchy sense). Note that the position of the singular points changes from iteration to iteration. An efficient use of the quadratures can be achieved by dividing the integration region into subintervals: a 24 point Clenshaw-Curtis integration was used on the intervals which contain singularities; in the remainder intervals the standard Gaussian rule was used. Less than 20 iteration were required to achieve a convergence to accuracy 10^{-5} on all points of the energy mesh in all our computations.

Below we present the results obtained for zero-temperature low-density neutron matter relevant to the physics of neutron star crusts. The density is fixed at the value $\rho_0/10$ ($\rho_0 = 0.17 \text{ fm}^{-3}$ is the nuclear saturation density) which corresponds to neutron Fermi momentum $p_F = 0.79 \text{ fm}^{-1}$. The on shell effective mass (which is an overall scaling factor and does not affect the physics off the mass shell) is arbitrarily fixed at the value $0.8m$, where m is the bare neutron mass. The density is chosen such that it is reasonable to assume that the dominant attractive interaction between neutrons is due to an exchange of neutral pions. Figure 2 displays the interaction kernel $K(\omega)$ as a function of the frequency. The kernel $K(\omega)$ has a Lorentzian shape at low and intermediate energies (characteristic also to spectral function $B(\mathbf{q}, \omega)$ for fixed values of $|q|$) with an excess contribution in the high-energy tail. Since the function $K(\omega)$ is an average of the pion spectral function over the momenta (with a certain weight from the pion-nucleon vertices) it is useful to examine the contribution of the spectral function $B(\omega, \mathbf{q})$ for fixed magnitude of the momentum transfer. The contribution from small momentum transfers $|q| \ll p_F$ is negligible since first, the amplitude of particle-hole excitations is generally small in this limit and second, because the integrand in Eq. (40) is weighted by the factor q^3 , with each pion-nucleon vertex contributing a power of q . The major contribution to the peak of $K(\omega)$ function originates from the momentum transfers $|q| \sim p_F$; in this regime the spectral function has a Lorentzian structure with the maximum coinciding with that of the $K(\omega)$ function. For large momentum transfers $|q| \leq 2p_F$ the spectral function is rather broad with the maximum shifted towards larger energies; the contribution to the high energy tail of the $K(\omega)$ function is due to the excitations with large momentum transfers.

Figure 3 shows the real and imaginary parts of the pairing amplitude and the wavefunction renormalization as a function of frequency. Note first that the $\omega \rightarrow 0$ limit of these functions is consistent with what is known from the on-shell physics. The real part of the gap function $\Delta_1^Q(\omega = 0)$ is of the order of MeV, as is the case for the pairing gaps deduced

using potential models. The real part of the wave-function renormalization $Z_1(\omega = 0)$ is *larger* than unity, i.e there is an enhancement of the density of states at the Fermi surface. This enhancement contracts the reduction of the density of states caused to the momentum-dependent effective mass $m^*/m < 1$. Finally, the imaginary parts of these functions vanish as they should. Perhaps the most striking feature seen in Fig. 3 is the energy range $\omega \sim 100$ MeV over which there are sizeable pairing correlations, which is in contrast to the phonon-exchange models where the functions vary on an energy scale which is an order of magnitude smaller. Another interesting feature is that the real and imaginary parts of the gap function develop a complicated structure over a wide energy range. In the low-energy domain, below the maximum of the function $K(\omega)$ at about 22 MeV, the real part of the gap function dominates the imaginary part: $|\Delta_1^Q(\omega)| > |\Delta_2^Q(\omega)|$. Beyond the maximum the opposite is true up to the energies $\omega \simeq 100$ MeV. A non-vanishing imaginary part $\Delta_2^Q(\omega)$ implies a finite decay time for the pairing correlations due to the coupling of the neutron quasiparticles to the pionic modes. Note that the RPA particle-hole renormalization acts to soften the pionic modes, but is not crucial to the finite life-time effects, which would be present for hard pions as well. The imaginary part of the wave-function renormalization $Z_2(\omega)$ implies, likewise, finite life-time for the normal quasiparticle excitation. It is worthwhile to note that the latter effect is *not* independent of the pairing correlations, since it emerges from a self-consistent solution of the coupled dynamics of the normal and anomalous sectors.

IV. CONCLUDING REMARKS

To summarize the main features of our model, one starts with a separation of the long and short range parts of the pairing interaction by explicitly including the pions and treating the short range correlations in terms of Landau parameters in the spirit of Migdal's theory of finite Fermi-systems. Thus, the pions emerge as the dominant bosonic degree of freedom of the model that cause the retardation of the interaction (which is the case at least in the low-density neutron matter treated here). One further carries out a renormalization of the pionic modes within the non-perturbative particle-hole (RPA) resummation scheme, which softens their spectrum, but has no effect on the retardation. The central quantities of the model are the Fock exchange self-energies, which couple the normal and anomalous propagators and give rise to off-mass-shell pairing correlations. In the final step the momentum dependence

of the Fock self-energies is integrated out by constraining the particle momenta to their Fermi-surfaces. The resulting coupled non-linear integral equations are solved numerically.

We find, surprisingly, that the paring correlations extend over a wide energy range, of the order 100 MeV, which is much larger than the range previously deduced for finite nuclei, where the interaction is due to an exchange of low-lying phonon modes. The real and imaginary parts of the gap function are of the same order of magnitude within this range and show a complicated behavior as functions of the energy. At low energies, the real part of the gap function dominates the imaginary part, i.e. the Fourier transform of the anomalous pair-correlation function in the time-domain shows a damped oscillatory behavior; the picture is opposite in the high energy regime, typically above tens of MeV, where the oscillations are damped out within a 'cycle'. Physically, the complex pairing gap implies finite life-time of the Cooper pairs due to the emission/absorption of the pionic modes. The real part of the wave-function renormalization (derived self-consistently with the gap equation) is larger than unity, i.e. implies an enhancement of the density of states; the non-vanishing imaginary part describes the damping of the normal quasiparticle excitations due to the coupling to the pion modes. Letting the energy to zero one recovers the on-shell (real) pairing amplitude and the (real) wave-function renormalization.

Extrapolating from the analysis of this paper it is clear that the meson-exchange picture of pairing (in the form formulated above) can be extended to treat problems which have been notoriously difficult to handle within the potential models. Such an extention could incorporate the dynamics of nucleon resonances, for example to elucidate the role of delta's in the effective retarded interaction or to deduce their pairing properties. Another promising direction is the extention of the model to the strange sector. This would allow us to access the pairing properties of the strange baryons that are stable in the interiors of compact stars (typically Σ and Λ hyperons, see Ref. [25]), the role of the kaon dynamics on the pairing properties of the strange baryons, etc. The model appears also suitable for treating the fermionic pair condensation of the baryons on the same footing with the Bose condensation of pions or kaons.

Acknowledgments

I would like to thank Herbert Müther and Peter Schuck for helpful discussions. This work has been supported by the Sonderforschungsbereich 382 of DFG.

- [1] P. Ring and P. Schuck, *The Nuclear Many Body Problem* (Springer-Verlag, New York, 1980).
- [2] A. B. Migdal, *Theory of Finite Fermi Systems and Applications to Atomic Nuclei* (Interscience, London, 1967).
- [3] S. O. Backman, G. E. Brown and J. A. Niskanen, Phys. Rept. **124**, 1 (1985), and references therein.
- [4] W. H. Dickhoff, A. Faessler, H. Müther and S. S. Wu, Nucl. Phys. **A405**, 534 (1983); W. H. Dickhoff, A. Faessler, J. Meyer ter Vehn and H. Müther, Phys. Rev. C **23**, 1154 (1981); W. H. Dickhoff and H. Müther, Nucl. Phys. **A473**, 394 (1987).
- [5] S. V. Babu and G. E. Brown, Ann. Phys. (N.Y.) **77**, 1 (1973).
- [6] J. Wambach, T. L. Ainsworth, and D. Pines, Nucl. Phys. **A555**, 128 (1993); T. L. Ainsworth, J. Wambach, and D. Pines, Phys. Lett. **B222**, 173 (1989).
- [7] H.-J. Schulze, J. Cugnon, A. Lejeune, M. Baldo, and U. Lombardo, Phys. Lett., **B375**, 1 (1996); H.-J. Schulze, A. Polls, and A. Ramos, Phys. Rev. C **63**, 044310 (2001).
- [8] J. Clark, C.-G. Källman, C.-H. Yang, D. Chakkalakal, Phys. Lett., **B61** 331 (1976); J. M. C. Chen, J. W. Clark, E. Krotschek, and R. A. Smith, Nucl. Phys. **A451**, 509 (1986); J. M. C. Chen, J. W. Clark, R. D. Davé, and V. V. Khodel, Nucl. Phys. **A555**, 59 (1993).
- [9] M. Baldo and A. Grasso, Phys. Lett. **B485** 115 (2000); P. Božek, Phys. Rev. C **62**, 054316 (2000); Phys. Lett. **B551**, 93 (2003); U. Lombardo, P. Schuck and W. Zuo, Phys. Rev. C **64**, 021301 (2001).
- [10] T. Alm, G. Röpke, A. Schnell, N. H. Kwong, and H. S. Köhler, Phys. Rev. C **53**, 2181 (1996); A. Schnell, G. Röpke and P. Schuck, Phys. Rev. Lett. **83**, 1926 (1999); G. Röpke and A. Schnell, Prog. Part. Nucl. Phys. **42**, 53 (1999); P. Božek Phys. Rev. C **65**, 034327 (2002).
- [11] A. Schwenk, B. Friman, and G. E. Brown, Nucl. Phys. **A713**, 191 (2003).
- [12] J. Kuckei, F. Montani, H. Müther, and A. Sedrakian, nucl-th/0210010.
- [13] C. Shen, U. Lombardo, P. Schuck, W. Zuo, and N. Sandulescu, nucl-th/0212027.

- [14] G. M. Eliashberg, Zh. Eksp. Teor. Fiz. **38**, 966 (1960) [Sov. Phys. JETP **11**, 696 (1960)].
- [15] A. Sedrakian, in *Proc. Int. Workshop Hirshegg '98, Nuclear Astrophysics*, edited by M. Buballa, W. Nörenberg, J. Wambach, and A. Wirzba, (GSI 1998) p. 54 [astro-ph/9801239].
- [16] J. Terasaki, F. Barranco, R. A. Broglia, E. Vigezzi, and P.-F. Bortignon, Nucl. Phys. **A697**, 127 (2002); J. Terasaki, F. Barranco, P.-F. Bortignon, R. A. Broglia, and E. Vigezzi, nucl-th/0109056.
- [17] A. V. Avdeenkov and S. P. Kamerdzhev, JETP Lett. **69**, 715 (1999); Yad. Fiz. **62**, 610 (1999). [Phys. Atom. Nucl. **62** (1999) 563.]; Phys Lett. **B459**, 423 (1999).
- [18] H. Kucharek and P. Ring, Z. Phys. A **339**, 23 (1991); F. B. Guimaraes, B. V. Carlson, and T. Frederico, Phys. Rev. C **54**, 2385 (1996); F. Matera, G. Fabbri, and A. Dellafiore, Phys. Rev. C **56**, 228 (1997).
- [19] G. Baym, H. A. Bethe, and C. J. Pethick, Nucl. Phys. **A175**, 225 (1971).
- [20] J. W. Negele and D. Vautherin, Nucl. Phys. **A207**, 298 (1973).
- [21] For a review see P. Haensel, in *Physics of Neutron Star Interiors*, D. Blaschke, N. K. Glendenning and A. Sedrakian (eds.), (Springer-Verlag, New York, 2001) p. 127.
- [22] J. W. Serene and D. Reiner, Phys. Rep. **101**, 221 (1983).
- [23] T. Ericson and W. Weise, *Pions and Nuclei*, (Clarendon Press, Oxford, 1988).
- [24] A. B. Migdal, Rev. Mod. Phys. **50**, 10 (1978).
- [25] N. K. Glendenning, *Compact Stars*, (Springer-Verlag, New York, 1st edition 1996, 2nd edition 2000); F. Weber, *Pulsars as Astrophysical Laboratories for Nuclear and Particle Physics* (IOP, Bristol 1999).

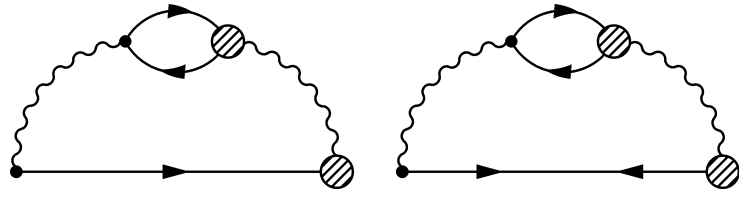


FIG. 1: Feynman diagrams illustrating the Fock exchange contributions to the normal (left graph) and anomalous (right graph) self-energies of baryons. The solid lines correspond to the fermions, the wavy lines - to the mesons. The blobs schematically indicate the RPA renormalized vertices.

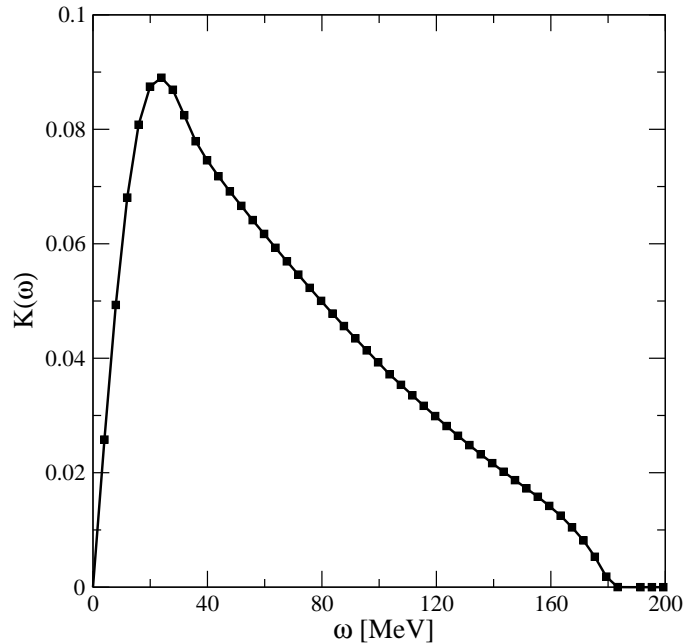


FIG. 2: The momentum-averaged (dimensionless) interaction kernel $K(\omega)$ in the RPA approximation to the pion spectral function and the pion-neutron vertex. The dots indicate the resolution of the frequency mesh used in the numerical calculations.

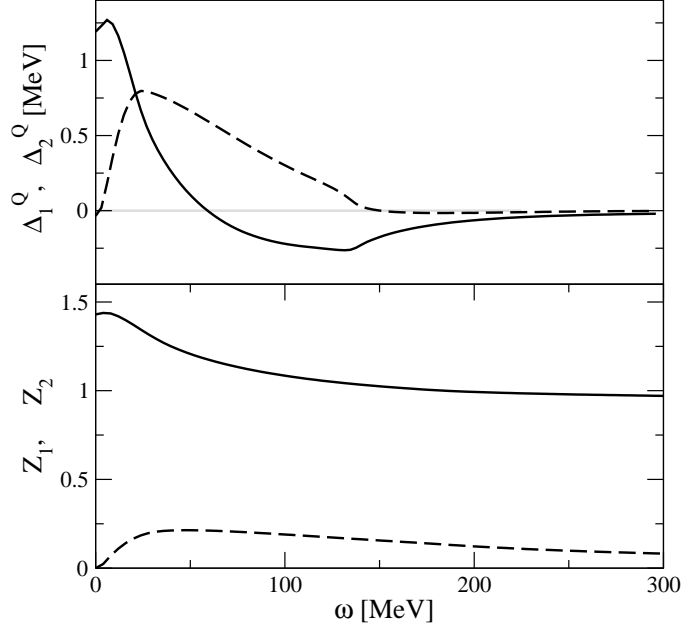


FIG. 3: Upper panel: The real and imaginary parts of the quasiclassical gap function $\Delta_1^Q(\omega)$ (solid line) and $\Delta_2^Q(\omega)$ (dashed line) respectively as a function of the off-mass-shell frequency. Lower panel: The real and imaginary parts of the wave-function renormalization $Z_1(\omega)$ (solid lines) and $Z_2(\omega)$ (dashed lines) respectively as a function of the off-mass-shell frequency.